Inorganic Chemistry

ARTICLE

pubs.acs.org/IC

Route to Metallacrowns: The Mechanism of Formation of a Dinuclear Iron(III)-Salicylhydroxamate Complex

Maria R. Beccia,[†] Tarita Biver,[†] Begoña García,*[,‡] José M. Leal,[‡] Fernando Secco,*[,†] and Marcella Venturini[†]

[†]Department of Chemistry and Industrial Chemistry, University of Pisa, Via Risorgimento 35, 56126 Pisa, Italy

[‡]Department of Chemistry, University of Burgos, Plaza Misael Bañuelos s/n., 09001 Burgos, Spain

Supporting Information

ABSTRACT: The equilibria and the kinetics of the binding of Iron(III) to salicylhydroxamic (SHA) and benzohydroxamic (BHA) acids have been investigated in aqueous solution (I = 1 M ($HClO_4$/$NaClO_4$), T = 298 K) using spectrophotometric and stopped-flow methods. Whereas Iron(III) forms a 1:1 complex (ML) with BHA, it forms both ML and M_2L complexes with SHA. The presence of M_2L in aqueous medium is corroborated by FTIR measurements. The reactive form of Iron(III) is the hydrolyzed species $FeOH^{2+}$, which binds to the O,O site in ML and to the O,O and O_P,N (P = phenolate) sites in M_2L, inducing full deprotonation of the latter. The reaction pathway is discussed in terms of a multistep mechanistic scheme in which the metal−ligand interaction is coupled to hydrolysis and self-aggregation steps of Iron(III). The observation and characterization of M_2L as a stable species is important because it contains the −Fe-O-N-Fe− sequence, which constitutes the repetitive motif of the SHA-based metallacrown ring and provides the rationale for 12-MC-4 metallacrowns. In the framework of this study, the kinetics of the Iron(III) dimerization and trimerization have also been investigated using the stopped-flow method to perform dilution jumps. The reaction scheme put forward involves two parallel steps ($FeOH^{2+}$ + $FeOH^{2+}$ and Fe^{3+} + $FeOH^{2+}$) that lead to formation of the $Fe_2(OH)_2^{4+}$ dimer and a slower step ($FeOH^{2+}$ + $Fe_2(OH)_2^{4+}$) to form the trimer species. The kinetics of the last step have been investigated here for the first time, and the results deduced indicate that, of the two possible trimer structures reported in the literature, $Fe_3(OH)_3^{6+}$ and $Fe_3(OH)_4^{5+}$, the latter prevails by far.

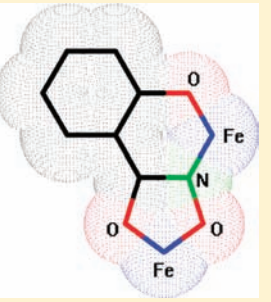

INTRODUCTION

Hydroxamic acids constitute an important family of bioligands. One of the first physiological roles of hydroxamic acids was associated to their use as siderophores (iron carriers).[1] These compounds, whether naturally occurring or synthetic, actually are able to coordinate Iron(III) with very high affinity;[2] the ability to act as metal chelators constitutes the basis for their use as flotation agents in extractive metallurgy[3,4] and for their employment in a range of biological applications.[5] These applications are not limited to solely metal binding, but rather hydroxamic acids also play an important role in enzyme inhibition[6,7] and have been employed as hypotensive,[8] antimalarial,[9−13] and anticancer agents.[14−17]

Primary hydroxamic acids bear two potentially acidic protons bound to the N and the O sites of the hydroxamate group (Scheme 1). However, they behave as monoprotic acids inasmuch as double deprotonation has never been observed, even at the highest OH^- concentration investigated.[18] Hydroxamic acids present two stereoisomers, Z and E, represented in Scheme 1.

The queries about which conformation, Z or E, is prevailing and whether hydroxamic acids may undergo N or O deprotonation have generated intense debate and numerous papers on these subjects[19] (and references therein). Whichever the preferred structure and the deprotonation process be, it is out of question that, to form a mononuclear complex, hydroxamic acids adopt the Z-conformation and the chelation process should involve O-deprotonation.[20]

Scheme 1

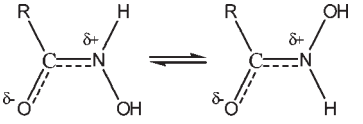

Z E

The presence of secondary coordinating residues at adjacent binding sites opens new perspectives in the coordination chemistry of hydroxamic acids. Salicylhydroxamate and α- and β-amino hydroxamates, combined with appropriate metal ions, give rise to important families of supramolecular compounds, the metallacrowns.[21−24] These species have been found to present interesting recognition properties,[25] not only toward cations (for instance through substitution of the core metals)[26] but also in the case of anions (for instance carboxylates).[27] More recently, metallacrowns have been found to function as single molecule magnets.[28,29]

Salicylhydroxamic acid contains both hydroxymate and phenolate donor atoms and is well suited to synthesize metallacrowns,

Received: May 25, 2011
Published: September 21, 2011

dx.doi.org/10.1021/ic201112j | Inorg. Chem. 2011, 50, 10152–10162

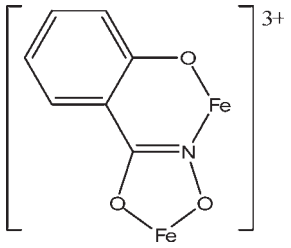

Figure 1. Structure assumed for the dinuclear complex of SHA that can represent the repetitive unit of a SHA-based metallacrown.

particularly in conjunction with highly charged metal ions (for instance, Iron(III)). SHA can in principle bind two Fe^{3+} ions, giving rise to a dinuclear, fully deprotonated complex (Figure 1), which constitutes the repetitive unit of an SHA-based metallacrown.[25] The structure of such a precursor complex was hypothesized by Pecoraro et al.,[25,30] but not found experimentally as an isolated entity. Actually, the experimental evidence on M^{2+}/SHA systems so far available denies full SHA deprotonation and formation of dinuclear SHA complexes. To this aim, it is worth mentioning that in a previous study on the mechanism of the Ni(II) binding to SHA,[31] we reported that divalent metal ions form only mononuclear complexes with SHA, whereas the N−H proton remains bound to the nitrogen atom irrespective of the strong polarization effect induced by the Ni^{2+} ion bound at the hydroxamate O,O site.

A wide range of metallacrowns that differ according to size and structure have been synthesized and characterized,[25,30] but their solution behavior needs further investigation. Recently, intensive thermodynamic studies concerning metal/aminohydroxamic acid systems have been carried out in aqueous solution that have enabled the acidity range, in which metallacrowns form and are stable, to be determined.[21] Moreover, studies on metal exchange at the metallacrown cavity have also been performed.[26] By contrast, information on the mechanism of the crown formation is rather scarce.

In this work, we have carried out a kinetic, thermodynamic, and IR spectroscopic investigation of the binding of Iron(III) to SHA and, for control purposes, to benzohydroxamic acid (BHA). The results show that a complex as that depicted in Figure 1 forms, and the thermodynamic and kinetic features of the process that lead to formation of this complex are worked out. Prior to the study of the binding of Iron(III) to the above hydroxamic acids, the kinetic behavior of solutions of $Fe(ClO_4)_3$ has been investigated at different $HClO_4$ concentrations to better understand the mechanism of the metal−ligand binding reaction, whose elucidation is rather complicated because of coupling with metal hydrolysis and self-aggregation steps.

EXPERIMENTAL SECTION

Chemicals. All chemicals were analytical grade (Aldrich). SHA and BHA solutions were prepared by weighing the appropriate amount of solid reagent (purity 99%) and dissolving it in doubly distilled water. Iron perchlorate, $Fe(ClO_4)_3 \cdot 6H_2O$, was dissolved in perchloric acid 0.34 M to prevent the Iron(III) hydroxide from precipitation. The Iron(III) concentration was measured by titration with EDTA. Perchloric acid and sodium perchlorate were used to attain the desired medium acidity and ionic strength, respectively.

Scheme 2

$$Fe^{3+} + H_2O \underset{}{\overset{K_H}{\rightleftharpoons}} FeOH^{2+} + H^+ \quad (1)$$

$$2FeOH^{2+} \underset{k_{-D}}{\overset{k_D}{\rightleftharpoons}} Fe_2(OH)_2^{4+} \quad (2)$$

$$FeOH^{2+} + Fe^{3+} + H_2O \underset{k'_{-D}}{\overset{k'_D}{\rightleftharpoons}} Fe_2(OH)_2^{4+} + H^+ \quad (2')$$

$$Fe_2(OH)_2^{4+} + FeOH^{2+} + H_2O \underset{k_{-T}}{\overset{k_T}{\rightleftharpoons}} Fe_3(OH)_4^{5+} + H^+ \quad (3)$$

Methods. The hydrogen ion concentrations of the aqueous solutions were determined by pH measurements performed by a Metrohm 713 instrument. A combined glass electrode was used, after the usual KCl bridge was replaced by 3 M NaCl to avoid precipitation of $KClO_4$. The electrode was calibrated with $HClO_4$ solutions of known concentration. This procedure enables the conversion of the pH-meter output into $-\log[H^+]$ values.

Absorption titrations were performed on a Perkin-Elmer Lambda 35 double beam spectrophotometer. Experiments were performed at 298 K and at $[H^+]$ = 1.0 to 0.01 M. Increasing amounts of the metal solution were added by a microsyringe to a ligand solution (SHA or BHA) already thermostatted in the measuring cell.

The kinetic experiments were performed on a MOS-300 Biologic stopped-flow mixing unit coupled to a spectrophotometric line by two optical guides. The UV radiation from a Xe lamp was passed through a Bausch and Lomb 338875 high intensity monochromator and then split into two beams. The reference beam was sent directly to a 1P28 photomultiplier. The output from the two photomultipliers was balanced before each shot. The acquisition system keeps a record of a number of data points ranging from 10 to 8000 with a sampling interval in the 50 μs to 10 s time scale. The kinetic curves were evaluated with the fitting package from AISN software (Jandel). Each shot was repeated at least 10 times, and the resulting kinetic curves were averaged via an accumulation procedure.

The complexes obtained from reactions of Iron(III) with BHA and SHA were also analyzed by attenuated total reflectance FTIR (FTIR-ATR) in solution using a Nexus 470 FTIR spectrophotometer from Nicolet Instrument Corporation. FTIR-ATR exploits the attenuation of the light reflected internally in a germanium nonabsorbing prism, because of energy absorption of an analyte in contact with the reflecting surface. To further enhance the attenuation, and consequently the absorption spectra, the prism has an oblong and trapezoidal shape to allow multiple internal reflections. The penetration depth of the absorption is of the order of a few micrometers and is a function of the wavelength, the angle of the incident beam, and the refractive index of both the sample and ATR prism. IR spectra of the two free ligands and of metal−ligand mixtures were recorded in different stoichiometric ratios. Contributions from water, reagents, and background were subtracted from the raw spectra.

RESULTS

Iron(III) Hydrolysis and Self-Aggregation. *Equilibria.* The process of Iron(III) hydrolysis and self-aggregation in aqueous solution has been investigated by UV/vis spectrophotometry at I = 1 M ($NaClO_4$) in the 0.01 to 1.0 M ($HClO_4$) acidity range. Lower acid concentrations can induce precipitation of $Fe(OH)_3$ and were avoided. The spectral behavior of $Fe(ClO_4)_3$ in 1.0 M $HClO_4$ (Supporting Information, Figures S1 and S2) clearly indicates that the only species present at $[H^+] \geq 1$ M is

dx.doi.org/10.1021/ic201112j |Inorg. Chem. 2011, 50, 10152–10162

Table 1. Reaction Parameters for Hydrolysis and Self-Aggregation Reactions of Iron(III); I = 1 M ($HClO_4/NaClO_4$), T = 298 K

K_H ($\times 10^{-3}$ M)	K_D($\times 10^3$ M^{-1})	K_T (M^{-1})	k_D ($\times 10^3$ M^{-1} s^{-1})	k_{-D} (s^{-1})	k_T (M^{-1} s^{-1})	k_{-T} (s^{-1})	k_D' [a] (M^{-1} s^{-1})	k_{-D}' [a] (s^{-1})
1.9	2.3	39	[b] 1.5 [c] 1.3	[b] 0.56	[c] 43	[c] 1.1	65	0.030

[a] Rate parameters for reaction (2′). [b] From kinetics at $[H^+]$ = 0.1 M. [c] From kinetics at $[H^+]$ = 0.01 M.

$Fe(H_2O)_6^{3+}$. In 0.01 M $HClO_4$ a remarkable *red shift* of the metal absorption band is observed (Supporting Information, Figure S3) and the Beer−Lambert law is no longer obeyed (Supporting Information, Figure S4), both findings revealing the presence of more than a single metal species. The analysis of the equilibrium and kinetic data suggests that, under the explored range of acid concentration (0.01 M ≤ $[H^+]$ ≤ 0.2 M), the main reactive processes are those reported in Scheme 2.

The absorbance of $Fe(ClO_4)_3$ solutions was measured at different metal and acid concentration, and the data have been subject to a multivariate nonlinear least-squares treatment as described in the Supporting Information. The values of the equilibrium constants of Scheme 2 reactions (1), (2), and (3), respectively K_H, K_D, and K_T, obtained by such an analysis are reported in Table 1. Here and in the following the subscripts D and T refer to the dimer and trimer respectively.

Kinetics. The kinetic behavior of the system (1)−(3) has been investigated using the stopped-flow method. The experiments have been performed in the concentration-jump mode by mixing a given volume of a $Fe(ClO_4)_3$ solution with an equal volume of water, both at the same desired pH and ionic strength value. Reaction (1) of Scheme 2 involves proton dissociation/association from a water molecule coordinated to Iron(III). This step reaches the equilibrium so rapidly that it cannot be monitored by the stopped-flow technique; the observed kinetic effects should then be related to self-aggregation steps. The experiments at $[H^+]$ = 1.0 M showed no kinetic effect. Actually, thermodynamic K values in Table 1 regarding the equilibria reveal that at $[H^+]$ = 1.0 M the Fe^{3+} ion species prevails by far. At $[H^+]$ = 0.1 M the kinetic curves are monoexponential (Figure 2A). This observation, along with the linear dependence of the reciprocal relaxation time versus the $[FeOH^{2+}]/([H^+] + K_H)$ ratio (Figure 2A, inset), allowed to rationalize the dynamic behavior of the system at $[H^+]$ ≥ 0.04 M on the basis of steps (1), (2), and (2′). Under these circumstances, step (3) can actually be disregarded, because the equilibrium data show that the trimer concentration becomes negligible at these relatively high acidity levels. Because reaction (1) is much faster than reactions (2) and (2′), the concentration dependence of the reciprocal relaxation time, $1/\tau_f$, is given by eq 4 (see Section 5 of the Supporting Information).

$$1/\tau_f = 4(k_D + k'_D[H^+]/K_H)(K_H/([H^+] + K_H))$$
$$[FeOH^{2+}] + (k_{-D} + k'_{-D}[H^+]) \quad (4)$$

where $[FeOH^{2+}]$ has been evaluated as described in Section 1 of the Supporting Information. The rate constants k_D, k_{-D}, k'_D and k'_{-D} (Table 1) have been evaluated by applying to eq 4 a nonlinear least-squares treatment using the values derived from the equilibria analyses.

The results obtained from the experiments at $[H^+]$ = 0.01 M are rather more complex. The exchange rate, evaluated using the data of Table 1, show that, under these circumstances, the extent of dimer formation through step (2′) is only 0.5%; hence,

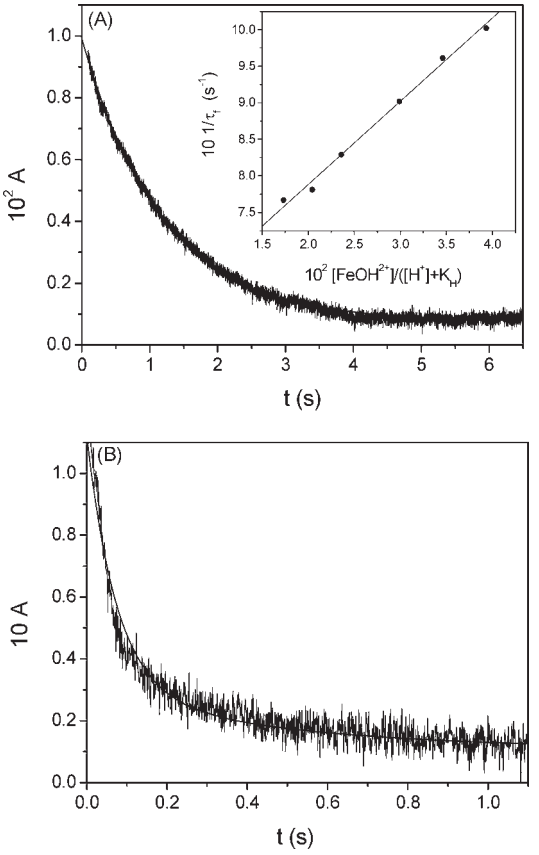

Figure 2. Stopped-flow experiments showing the kinetic behavior of $Fe(ClO_4)_3$ solutions upon dilution jumps at I = 1 M ($HClO_4/NaClO_4$) and T = 298 K: (A) C_M = 0.11 M, $[H^+]$ = 0.1 M; (B) C_M = 0.036 M, $[H^+]$ = 0.01 M. Note that, whereas the curve (A) is perfectly monoexponential, curve (B) deviates from the monoexponential behavior shown by the continuous line. Inset: plot of the kinetic data according to eq 4.

at $[H^+]$ = 0.01 M, this step can be neglected. Nevertheless, the kinetic curves become biexponential (Figure 2B). The change of behavior should be ascribed to involvement of step (3) which, for $[H^+]$ < 0.04 M, gives a noticeable contribution to the observed kinetics. The usual data treatment, where the fast relaxation is analyzed as a fast equilibrium not affected by the slow effect, could not be applied here because the two effects ($1/\tau_f$ and $1/\tau_s$) are only poorly separated on the time scale (Table 2). Hence, a whole kinetic analysis of the coupled reactions was applied to Scheme 2. The Castellan's method[32] was employed, which makes use of the exchange rates to obtain the concentration dependence of the fast ($1/\tau_f$) and slow ($1/\tau_s$) relaxation times (see Supporting Information). However, instead of analyzing the two expressions separately to obtain the rate constants of steps (2) and (3), these were evaluated by a combination of relaxation times (eqs 5 and 6), according to a procedure developed in our

dx.doi.org/10.1021/ic201112j |*Inorg. Chem.* 2011, 50, 10152–10162

Table 2. Dependence of the Relaxation Times, $1/\tau_f$ and $1/\tau_s$ for the Self-Aggregation Reaction of Iron(III) on the Hydrogen Ion Concentration; C_M = 0.1 M, I = 1 M ($HClO_4$/$NaClO_4$), T = 298 K

$[H^+]$ (M)	$1/\tau_f$ (s^{-1})	$1/\tau_s$ (s^{-1})
0.01	13	2.2
0.02	4.3	1.7
0.03	2.3	1.5
0.04	1.4	
0.05	1.3	
0.06	1.1	
0.08	0.83	
0.10	0.77	
0.13	0.78	
0.16	0.85	
0.20	1.1	

laboratory,[33] which has been adapted to the present system (see Section 2 of the Supporting Information):

$$1/\tau_f + 1/\tau_s = (4\chi_D + \chi_T)C_M + (\chi_{-D} + \chi_{-T}) \quad (5)$$

$$1/\tau_f + 1/\tau_s = 6\chi_D\chi_T C_M^2 + 4\chi_D\chi_{-T}C_M + \chi_{-D}\chi_{-T} \quad (6)$$

where χ_D, χ_T, χ_{-D}, and χ_{-T} are apparent rate parameters linked to the rate constants of the individual steps (2) and (3) as shown below. A plot according to eq 5 is shown in Figure 3A. The slope and intercept of the straight line interpolating the data points provide $(4\chi_D + \chi_T) = (139 \pm 2)\ M^{-1}\ s^{-1}$ and $(\chi_{-D} + \chi_{-T}) = (1.7 \pm 0.2)\ s^{-1}$, respectively. On the other hand, the parabolic function represented in Figure 3B, which corresponds to eq 6, has enabled us to obtain the parameters $6\chi_D\chi_T = (1.4 \pm 0.1) \times 10^3\ M^{-2}\ s^{-2}$, $4\chi_D\chi_{-T} = (1.4 \pm 2) \times 10^2\ M^{-1}\ s^{-2}$ and $\chi_{-D}\chi_{-T} = (1 \pm 0.7)\ s^{-2}$. Combination of these parameters yields the apparent rate constants. The latter are linked to the individual rate constant of Scheme 2 by the relationships $k_D = \chi_D K_H^2/(K_H + [H^+])^2$, $k_T = \chi_T K_H/(K_H + [H^+])$, $k_{-D} = \chi_{-D}$ and $k_{-T} = \chi_{-T}/[H^+]$. The rate constants evaluated at $[H^+]$ = 0.01 M are reported in Table 1. Special attention has been paid to investigate the dependence on $[H^+]$ of the reverse step of reaction (3). For this purpose, a set of experiments was devised in which a solution containing the preformed trimer was mixed with given amounts of $HClO_4$ and the time constant of the trimer decomposition, $1/\tau_{diss}$, has been measured for each $[H^+]$ value. Figure 4 shows that $1/\tau_{diss}$ is directly proportional to $[H^+]$. This result will be discussed later in connection with the structure of the trimer.

Besides the above-described kinetic processes, a very slow reaction was detected on the time scale of hours (Supporting Information, Figure S5). This reaction, monitored by classical spectrophotometry, was ascribed to formation of more complex Iron(III) aggregates, and was not further investigated.

Reactivity of Iron(III) with BHA and SHA. *Equilibria.* The equilibria of the interaction of Iron(III) with BHA and SHA have been investigated by spectrophotometric titrations at I = 1 M ($NaClO_4$) in the 0.01 M ≤ $[HClO_4]$ ≤ 1 M acidity range. All titrations were performed under conditions of metal excess to exclude the formation of complexes such as ML_2 or ML_3.

Iron(III)/BHA System. Titration of BHA with Iron(III) under $C_M/C_L \geq 10$ conditions do provide monophasic binding isotherms

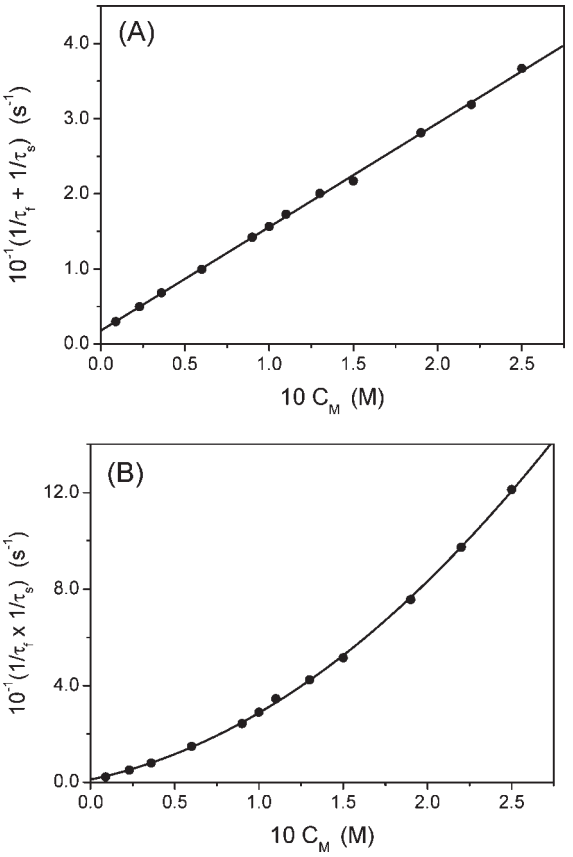

Figure 3. Dependence of $1/\tau_f + 1/\tau_s$ (A) and $1/\tau_f \times 1/\tau_s$ (B) versus C_M at $[H^+]$ = 0.01 M, I = 1 M ($HClO_4$/$NaClO_4$) and T = 298 K.

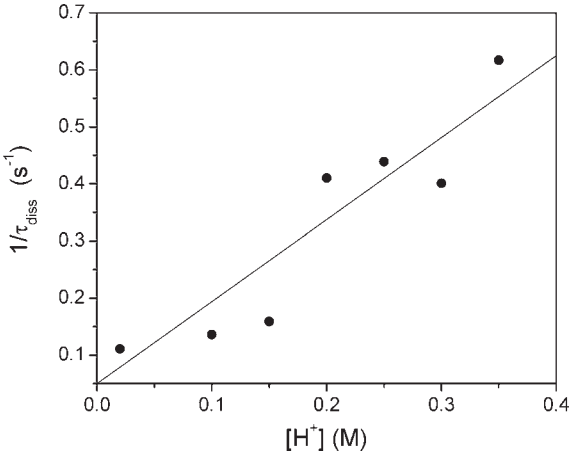

Figure 4. Dependence of the rate constant of trimer decomposition on the hydrogen ion concentration; I = 1 M ($HClO_4$/$NaClO_4$) and T = 298 K.

(Figure 5A), which represent the formation of 1:1 complexes (denoted in total as ML_T) from reaction between the free iron (M_f) ($[M_f] = [Fe^{3+}] + [FeOH^{2+}] + 2[D] + 3[T]$) and the free ligand ($L_f$) where $[L_f] = [H_2L]$, according to the apparent reaction 7

$$M_f + L_f \overset{K_{lapp}}{\rightleftarrows} ML_T \quad (7)$$

dx.doi.org/10.1021/ic201112j |*Inorg. Chem.* 2011, 50, 10152–10162

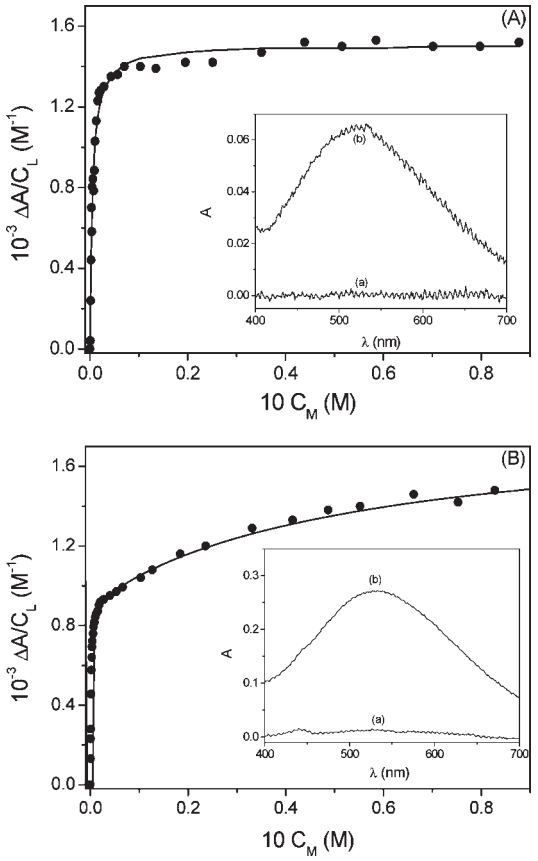

Figure 5. Binding isotherms for the interaction of Iron(III) with hydroxamic acids with related insets showing the spectral change induced by complex formation; I = 1 M ($HClO_4$/$NaClO_4$) and T = 298 K: (A) [BHA] = 2.5 × 10^{-4} M, [H^+] = 0.1 M, inset: (a) C_M = 0 M, (b) C_M = 1.7 × 10^{-1} M; (B) [SHA] = 2.5 × 10^{-4} M, [H^+] = 0.022 M, inset: (a) C_M = 0 M, (b) C_M = 1.7 × 10^{-1} M.

The binding isotherms have been analyzed according to eq 8

$$\Delta A/C_L = \Delta\varepsilon K_{1app} C_M/(1 + K_{1app} C_M) \quad (8)$$

where $\Delta A = (A - A_0)$, $\Delta\varepsilon = (\varepsilon_{ML} - \varepsilon_L - \varepsilon_M)$, and K_{1app} is the equilibrium constant of reaction 7. The dependence of K_{1app} on [H^+] displays the rather unusual behavior shown in Figure 6. Such a dependence can be rationalized on the basis of a mechanism that involves the coupling between complex formation and hydrolysis/aggregation of Iron(III). At [H^+] values less than 0.025 M, both the dimer and the trimer formation subtract metal to complexation, so K_{1app} decreases as [H^+] tends to zero. At the highest [H^+] values, the complex formation is also hindered because the concentration of the reactive species, $FeOH^{2+}$, is reduced. Moreover, for [H^+] ≥ 1 M BHA tends to form the $BHAH^+$ species,[34] which is reluctant to metal binding. The outcome is that the dependence of K_{1app} on [H^+] displays a maximum. The [H^+] dependence of K_{1app} is given by eq 9.

$$K_{1app} = \alpha_{FeOH} K_{ML} \quad (9)$$

where α_{FeOH} = [FeOH]/[M_f] and K_{ML} is the equilibrium constant of reaction 10 (see Section 4 of the Supporting Information).

$$FeOH^{2+} + H_2L \overset{K_{ML}}{\rightleftarrows} FeHL^{2+} + H_2O \quad (10)$$

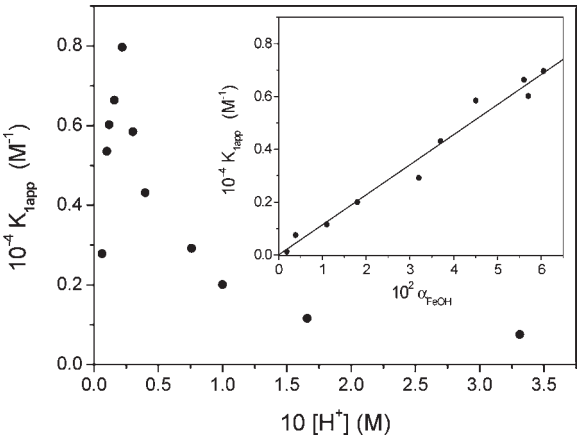

Figure 6. Dependence of the apparent binding constant, K_{1app}, for the Iron(III)/BHA system on [H^+] at I = 1 M ($HClO_4$/$NaClO_4$) and T = 298 K; inset: dependence of K_{1app} on α_{FeOH}, the molar fraction of $FeOH^{2+}$ ion.

A plot of K_{1app} versus α_{FeOH} according to eq 9 yields a straight line (inset of Figure 6) whose slope provides the K_{ML} value reported in Table 3.

Iron(III)/SHA System. The thermodynamic study of the Iron(III)/SHA system reveals two different sorts of behavior depending on the medium acidity. For high [H^+] values the binding isotherms are monophasic, as those obtained for the Iron(III)/BHA system (Supporting Information, Figure S6), whereas they become biphasic for lower [H^+] values, indicating that a further binding step becomes operative under such conditions (Figure 5B). This step is compatible with the formation of a dinuclear complex. The titration curves have been analyzed using eq 11,[35] where $\Delta\varepsilon_1 = (\varepsilon_{MLT} - \varepsilon_{Lf} - \varepsilon_{Mf})$, $\Delta\varepsilon_2 = (\varepsilon_{M2LT} - \varepsilon_{Lf} - \varepsilon_{Mf})$, and K_{2app} is the equilibrium constant for formation of M_2L_T from reaction of ML_T with M_f, that is, $K_{2app} = [M_2L_T]/[ML_T][M_f]$. Note that, in the case of monophasic behavior, eq 11 is reduced to eq 8.

$$\Delta A/C_L = (\Delta\varepsilon_1 K_{1app} C_M + \Delta\varepsilon_2 K_{1app} K_{2app} C_M{}^2)/(1 + K_{1app} C_M + K_{1app} K_{2app} C_M{}^2) \quad (11)$$

The values of both K_{1app} and K_{2app} depend on [H^+], as shown in Figure 7A and 7B, respectively. The trend of K_{1app} is similar to that observed for the Iron(III)/BHA system and has been analyzed using eq 11, now being [L_f] = [H_3L] and K_{ML} = [FeH_2L^{2+}]/([$FeOH^{2+}$][H_3L]), while the trend of K_{2app} has been analyzed using eq 12 which has been derived according to reaction 13.

$$K_{2app} = K_{M2L}\alpha_{FeOH}/[H^+] \quad (12)$$

$$FeH_2L^{2+} + FeOH^{2+} \overset{K_{M2L}}{\rightleftarrows} Fe_2L^{3+} + H_3O^+ \quad (13)$$

A plot of [H^+] × K_{2app} versus α_{FeOH} is linear (Figure 7B inset), and its slope yields the value of K_{M2L}, the equilibrium constant of reaction 13. The stoichiometry of reaction 13 is also confirmed by the kinetic results which show (Figure 11) that the decomposition of one Fe_2L^{3+} ion requires one proton. The values of K_{ML} and K_{M2L} are reported in Table 3.

Kinetics. The kinetics of the Iron(III) binding to BHA and SHA have been investigated under pseudo-first order conditions

dx.doi.org/10.1021/ic201112j |*Inorg. Chem.* 2011, 50, 10152–10162

Table 3. Reaction Parameters for Complex Formation Reactions of Iron(III) with Benzohydroxamic Acid (BHA) and Salicylhydroxamic Acid (SHA); I = 1 M ($HClO_4$/$NaClO_4$), T = 298 K

	K_{ML} ($\times 10^5$ M^{-1})	K_{M2L} ($\times 10^2$ M^{-1})	k_1 ($\times 10^4$ M^{-1} s^{-1})	k_{-1} (s^{-1})	$K_D k_2$ ($\times 10^7$ s^{-1})	$K_D K_2 k_3/K_{ML}$ (s^{-1})	$k_{-3}K_{CH}$ (M^{-1} s^{-1})
BHA	1.1		1.8	0.12			
SHA	1.3	3.6	[a]1.4	[a]0.004			
			[b]1.6		1.1	95	1.6

[a] From data at $[H^+]$ = 1 M. [b] From data at $[H^+]$ = 0.1 M.

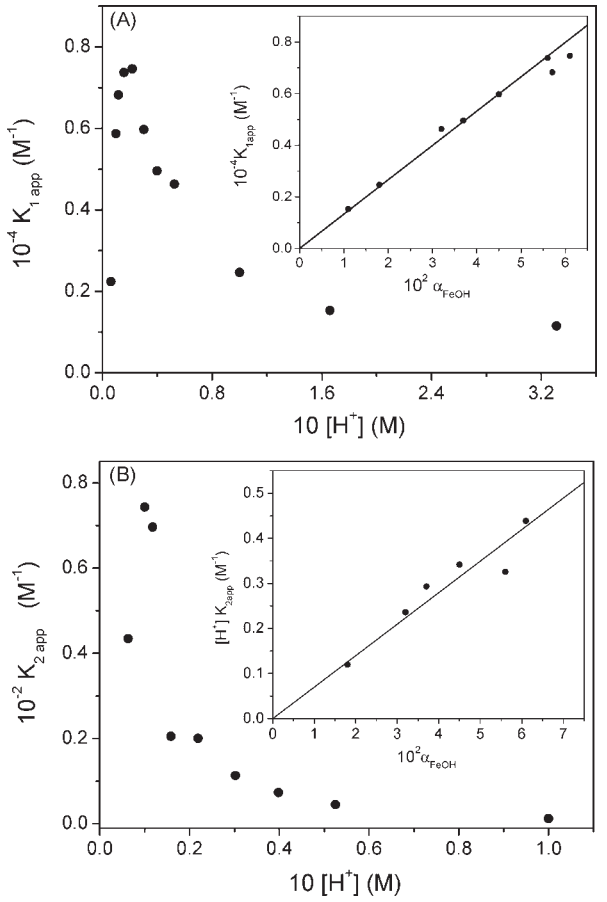

Figure 7. Dependence of the apparent binding constants, K_{1app} and K_{2app}, for the Iron(III)/SHA system on $[H^+]$ at I = 1 M ($HClO_4$/$NaClO_4$) and T = 298 K; (A) plot of K_{1app} versus $[H^+]$, inset: dependence of K_{1app} on α_{FeOH}. (B) Plot of K_{2app} versus $[H^+]$, inset: dependence of $[H^+] \times K_{2app}$ on α_{FeOH}.

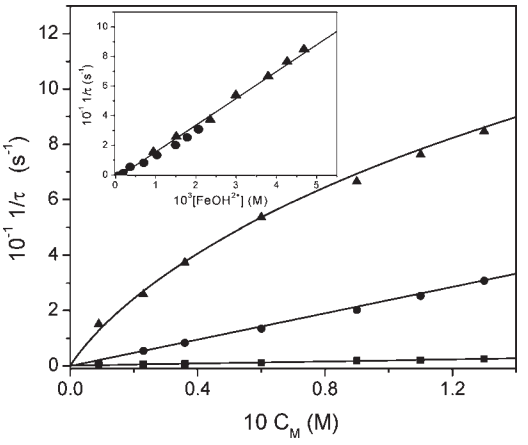

Figure 8. Dependence of $1/\tau$ versus C_M at different $[H^+]$ values for the Iron(III)/BHA system at I = 1 M ($HClO_4$/$NaClO_4$) and T = 298 K; [BHA] = 2.5×10^{-4} M, $[H^+]$ = 1 M ■, 0.1 M ●, 0.01 M ▲. The inset represents the dependence of $1/\tau$ on $[FeOH^{2+}]$, calculated at all acidities by the relationship $[FeOH^{2+}] = \alpha_{FeOH}\, C_M$.

($C_M/C_L \geq 10$) using the stopped-flow method. For both systems the complex formation process is coupled with the Iron(III) hydrolysis and self-aggregation processes.

Iron(III)/BHA System. The kinetic traces obtained for the binding of Iron(III) to BHA are monoexponential in the $[H^+]$ = 0.1 to 1.0 M range (Supporting Information, Figure S7). The dependence of $1/\tau$ on C_M is linear at $[H^+]$ = 1.0 and 0.1 M (Figure 8). Note that the rate of reaction largely increases upon reducing $[H^+]$ from 1.0 to 0.1 M, in parallel with the increase of $[FeOH^{2+}]$ induced by the $[H^+]$ reduction. This observation indicates that $FeOH^{2+}$ is the reactive species, while the hexaaquoion Fe^{3+}, although present in large excess at both acidity levels, reacts with BHA to a negligible extent. That the reacting species is $FeOH^{2+}$ is also confirmed by the rate dependence on C_M at $[H^+]$ = 0.01M. Here, a downward deviation from linearity can be observed in the $1/\tau$ versus C_M plot (Figure 8). Such a deviation depends on the behavior of α_{FeOH}, which, at $[H^+]$ = 0.01M, decreases as the metal ion content is raised, owing to the contribution of the self-aggregation steps which subtract the $FeOH^{2+}$ reactive species to the binding process. It can then be assumed that the prevailing binding step for BHA is represented by reaction 10. Bearing in mind that reaction 10 is coupled to the hydrolysis and self-aggregation steps through the common species $FeOH^{2+}$ and that $[M_f] \approx C_M$, it follows that the concentration dependence of the relaxation time of the complex formation reaction is given by the relationship 14

$$1/\tau = k_1[FeOH^{2+}] + k_{-1} \qquad (14)$$

where k_1 and k_{-1} are respectively the forward and reverse rate constants of reaction 10. The inset of Figure 8 shows the $1/\tau$ versus $[FeOH^{2+}] = \alpha_{FeOH}\, C_M$ plot. Now all the data points lie on a single straight line according to eq 14, which provides the k_1 and k_{-1} values collected in Table 3.

Iron(III)/SHA System. This system exhibits a more complex kinetic behavior. At $[H^+]$ = 1.0 M, the kinetics are monoexponential (Figure 9A) provided that $C_M \leq 0.04$ M. The metal concentration dependence of the relaxation time is linear (Figure 10A). The kinetic behavior is similar to that displayed by the Iron(III)/BHA system under similar conditions and is ascribed to formation of a mononuclear complex between Iron(III) and SHA.

The behavior becomes more complex at $[H^+]$ = 0.1 M and even more at $[H^+]$ = 0.01 M (Figure 9B). Actually, the system displays now two kinetic effects, in contrast with the behavior of

dx.doi.org/10.1021/ic201112j |*Inorg. Chem.* 2011, 50, 10152–10162

the Fe/BHA system where, under similar conditions, simple kinetics are observed. The metal concentration dependence of the fastest of the two effects is parabolic (Figure 10B), revealing the occurrence of a second-order binding step with respect to the metal ion. On the other hand, the rate constant of the slow kinetic effect displays a linear dependence on C_M (Figure 10C).

The kinetic features of the Iron(III)/SHA system can be rationalized on the basis of the reaction Scheme 3, where H_3L denotes the uncharged triprotonated SHA species.

Since the two effects are widely separated on the time scale, the fast effect has been analyzed separately from the slow one, whereas in the analysis of the slow effect, reactions (15) and (16) are regarded as pre-equilibrium steps. The expressions of the relaxation times for the two kinetic effects (eqs 18 and 19) have been derived as described in the Supporting Information. The values of the parameters obtained by this analysis are reported in Table 3.

$$1/\tau_{fast} = k_1[FeOH^{2+}] + K_D k_2[FeOH^{2+}]^2 + (k_{-1} + K_C k_{-2}[FeOH^{2+}])/(1 + K_C[FeOH^{2+}])$$
$$\text{where} \quad K_C = [Fe_2OHH_2L^{4+}]/[FeH_2L^{2+}][FeOH^{2+}] \qquad (18)$$

$$1/\tau_{slow} = K_D K_2 k_3[FeOH^{2+}]^2/(1 + K_1[FeOH^{2+}] + K_2 K_D[FeOH^{2+}]^2) + k_{-3}K_{CH}[H^+]/(1 + K_{CH}[H^+])$$
$$\text{where} \quad K_{CH} = [Fe_2HL^{4+}]/[Fe_2L^{3+}][H^+] \qquad (19)$$

The fast effect has been analyzed according to eq 18. Since the intercept of the parabolic function expressing $1/\tau_{fast}$ versus $[FeOH^{2+}]$ is close to zero (Figure 10B), the third term of the right-hand side in eq 18 has been neglected.

Concerning the slow effect, the linear dependence $1/\tau_{slow}$ versus $[FeOH^{2+}]$ (Figure 10C) indicates that the inequality $K_1[FeOH^{2+}] \gg 1 + K_2K_D[FeOH^{2+}]^2$ holds in the denominator of the first term of eq 19. This conclusion is confirmed by the values of the equilibrium data, which show that the above inequality is satisfied over the full $[FeOH^{2+}]$ range investigated. Moreover, the intercept of the plot of Figure 10C is very small; hence, the contribution of the reverse step of reaction (17) cannot be evaluated using eq 19. Therefore, the slow reaction has been investigated in the reverse direction by mixing the pre-formed 2:1 complex in the stopped flow apparatus with known amounts of $HClO_4$ (Supporting Information, Figure S8). The dependence of the time constant on the acidity level is shown in Figure 11. The linear behavior observed is in good agreement with reaction (17) and indicates that the inequality $K_{CH}[H^+] \ll 1$ holds in eq 19 and so the slope of the straight line of Figure 11 yields $k_{-3}K_{CH}$.

FTIR Experiments. Infrared spectra of aqueous solutions of BHA and SHA have been recorded at pH = 1.66 and I = 1 M. Moreover, the spectra of the ligand and Iron(III) mixtures in the stoichiometric ratios C_M/C_L = 1 and 2 have been recorded also at pH = 1.66 ($[H^+]$ = 0.022 M), where the extent of complex formation is highest. Concerning the Iron(III)/BHA system, Figure 12A shows that the band corresponding to the N−H vibrational frequency (3300 cm^{-1})[36,37] does not display any remarkable change on going from BHA alone to mixtures of BHA and $Fe(ClO_4)_3$. In particular, the spectra of solutions in which both the metal and the ligand are mixed in the ratios C_M/C_L = 1 and C_M/C_L = 2 are very similar. Comparison of the spectra

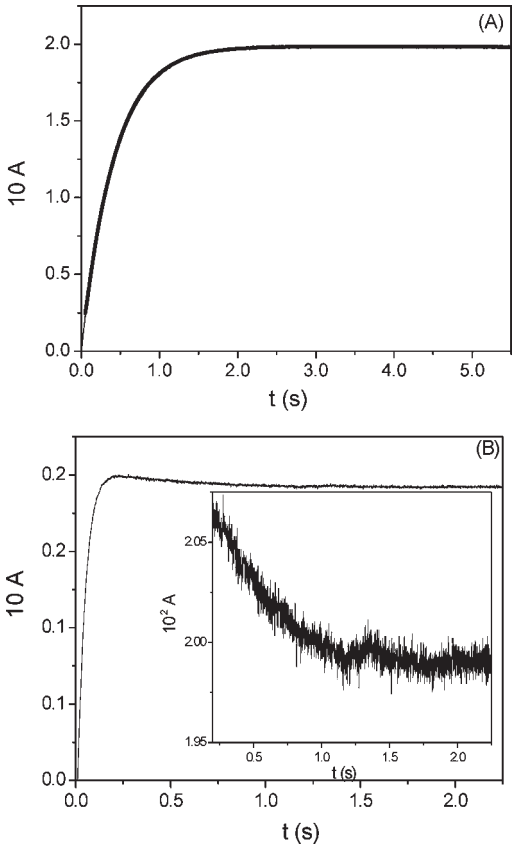

Figure 9. Stopped-flow traces recorded at λ = 532 nm upon mixing SHA 2.5 × 10^{-4} M and $Fe(ClO_4)_3$ 9.0 × 10^{-3} M at I = 1 M ($HClO_4$/$NaClO_4$) and T = 298 K; (A) $[H^+]$ = 1.0 M (monoexponential trace), (B) $[H^+]$ = 0.01 M (biexponential trace). The inset shows the slowest of the two effects on a magnified scale.

indicates that Iron(III) is chelated by BHA through the O,O oxygen atoms, and that only the 1:1 complex is formed.

Concerning the Iron(III)/SHA system, comparison of the spectrum of SHA alone with those of the C_M/C_L = 1 and C_M/C_L = 2 mixtures (Figure 12B) shows that, like in the case of the Iron(III)/BHA control system, Iron(III) binds to SHA through the O,O sites. Moreover, comparison of the spectral behavior of the C_M/C_L = 1 and C_M/C_L = 2 mixtures reveals that the bands corresponding to the phenol O_P−H (3463 cm^{-1}) and N−H stretching (3300 cm^{-1}),[36,37] which for C_M/C_L = 1 mixtures are well evident (although overlapped) between 3000 and 3400 cm^{-1}, become reduced to a large extent for the C_M/C_L = 2 mixture. This outcome indicates that the second Iron(III) ion in the binuclear complex is bound to SHA through the O_P,N site.

DISCUSSION

Iron(III) Hydrolysis and Self-Aggregation. The value of the equilibrium constant for the dimer formation, k_D/k_{-D} = 2.7 × 10^3 M, obtained in this study from kinetics compares satisfactorily with that from the spectrophotometric titration (Table 1), and both values compare pretty well with the literature data.[38] Actually, our equilibrium constant for dimerization, K_D, can be converted to the value quoted by Baes and Mesmer[38] (K_D^{BM} = 2.3 × 10^{-3} M at I = 1 M and 25 °C) using the relationship $K_D^{BM} = [Fe_2O^{4+}][H^+]/[Fe^{3+}]^2 = K_D \times K_H^2$. By application of such an equation we obtain K_D^{BM} = 2.7 × 10^{-3} M.

dx.doi.org/10.1021/ic201112j |*Inorg. Chem.* 2011, 50, 10152–10162

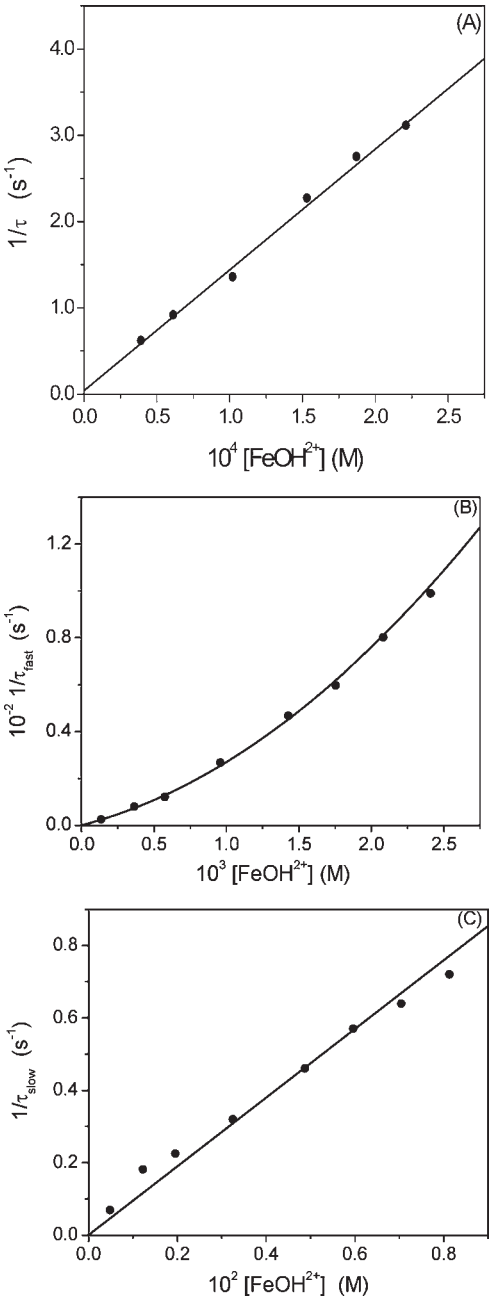

Figure 10. Dependence of the relaxation time on $[FeOH^{2+}]$ for the Iron(III)/SHA system under different acidity conditions at I = 1 M ($HClO_4/NaClO_4$) and T = 298 K; (A) $[H^+]$ = 1.0 M (single effect); (B) $[H^+]$ = 0.1 M (fast effect); (C) $[H^+]$ = 0.1 M (slow effect).

Application of the Davies equation[39] with B = 0.1 to a bimolecular reaction in which the charge product of the reactant is +4 shows that the rate constant ratio, $k_{I=3.0M}/k_{I=1.0M}$ = 0.5, is in good agreement with the 0.46 ratio obtained by dividing the k_D value published by Sommer and Margerum (6.4×10^2 M s^{-1}, I = 3.0 M, T = 298 K)[40] by our value. On the other hand, the same procedure shows that our rate constant k_D (Table 1) is somewhat higher than the 8.1×10^2 M^{-1} s^{-1} value derived by conversion at I = 1 M of the Wendt datum[41] (4.5×10^2 M^{-1} s^{-1}, I = 0.6 M, T = 298 K) using the Güntelberg equation.[42] Concerning the reverse step, our value of k_{-D} should be considered in agreement with the value of 0.42 s^{-1} reported by Po and Sutin,[43] who investigated the dimer dissociation, but somewhat higher than that obtained by Sommer and Margerum.[40]

Scheme 3

Fast effect:

$$FeOH^{2+} + H_3L \underset{k_{-1}}{\overset{k_1}{\rightleftharpoons}} FeH_2L^{2+} + H_2O \qquad (15)$$

K_D ⇅ $FeOH^{2+}$ $\qquad$ K_C ⇅ $FeOH^{2+}$

$$Fe_2(OH)_2^{4+} + H_3L \underset{k_{-2}}{\overset{k_2}{\rightleftharpoons}} Fe_2OHH_2L^{4+} + H_2O \qquad (16)$$

Slow effect:

$$Fe_2OHH_2L^{4+} \underset{k_{-3}}{\overset{k_3}{\rightleftharpoons}} Fe_2HL^{4+} + H_2O \overset{1/K_{CH}}{\rightleftharpoons} Fe_2L^{3+} + H_3O^+ \qquad (17)$$

Concerning the process of formation/dissociation of the trimer, Table 1 shows the excellent agreement between the value of K_T obtained from static titrations and that obtained from kinetics as k_T/k_{-T}. Two possible structures have been assumed for the trimer species,[40] namely, $Fe_3(OH)_4^{5+}$ and $Fe_3(OH)_3^{6+}$ (Scheme 4).

The linear dependence of the trimer dissociation rate on $[H^+]$ (Figure 4) shows that the prevailing form of the trimer is $Fe_3(OH)_4^{5+}$, since the decomposition of $Fe_3(OH)_3^{6+}$ would had been acidity independent. However, the direct encounter of $Fe_2(OH)_2^{4+}$ with $FeOH^{2+}$ (which are involved in reaction (3)) would give rise to $Fe_3(OH)_3^{6+}$, whereas the formation of $Fe_3(OH)_4^{5+}$ would require the improbable encounter of $Fe_2(OH)_2^{4+}$ with the doubly hydrolyzed monomer $Fe(OH)_2^+$ present in extremely low amounts. Alternatively, $Fe_3(OH)_4^{5+}$ could be formed by the evolution of $Fe_3(OH)_3^{6+}$. If this were the case, eq (3) should be rewritten in the more detailed form corresponding to the reaction sequence eq 20.

$$Fe_2(OH)_2^{4+} + FeOH^{2+} + H_2O \rightleftarrows Fe_3(OH)_3^{6+}$$

$$+ H_2O \overset{K_B}{\rightleftarrows} Fe_3(OH)_4^{5+} + H^+ \qquad (20)$$

According to sequence 20, the rate constant for the process of trimer dissociation, $1/\tau_{diss}$, would be expressed by eq 21, where K_B is the acid dissociation constant of the $Fe_3(OH)_3^{6+}$ ion:

$$1/\tau_{diss} = k_T[H^+]/(K_B + [H^+]) \qquad (21)$$

The linear dependence of $1/\tau_{diss}$ versus $[H^+]$ (Figure 4) indicates that $K_B \gg [H^+]$ and that $[Fe_3(OH)_4^{5+}] \gg [Fe_3(OH)_3^{6+}]$. Finally, concerning the very slow step observed (Supporting Information, Figure S5), it can be ascribed to formation of more extended aggregates, whose structures we are unable to predict. We only could guess that they could form by addition of the $FeOH^{2+}$ ion to an already formed aggregate, since the linkage of two identical aggregates is disfavored by the electrostatics of the system. For instance, the linkage of two dimers to give a tetramer (charge product = +16) would experience a repulsion effect larger than that corresponding to the union of a trimer with $FeOH^{2+}$ (charge product = +10). Actually, simple calculations based on the electrostatic theory of electrolytes[44] show that the increased repulsion results in a free energy penalty of 3.3 kcal mol^{-1} when the charge product rises from +10 to +16.

dx.doi.org/10.1021/ic201112j |*Inorg. Chem.* 2011, 50, 10152–10162

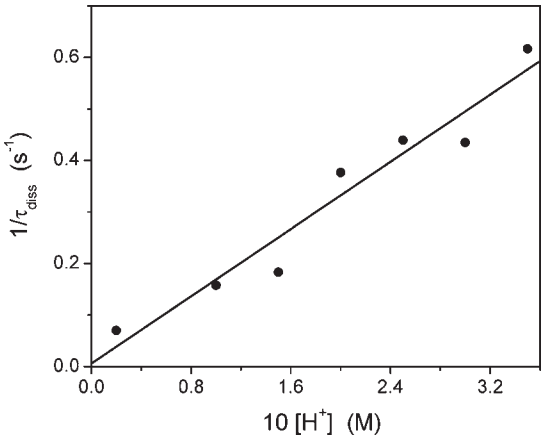

Figure 11. Dependence of the rate dissociation, $1/\tau_{diss}$, on the hydrogen ion concentration for the Iron(III)/SHA system at $I = 1$ M ($HClO_4$/$NaClO_4$) and $T = 298$ K.

Complex Formation of Iron(III) with BHA and SHA. *Iron(III)/BHA.* It has been found that the K_{ML} value reported in Table 3 for the 1:1 Iron(III)/BHA complex compares excellently with $K_{ML} = Q_f/K_H = 1.0 \times 10^5\ M^{-1}$ derived from $Q_f = [FeHL][H]/[Fe][H_2L] = 1.7 \times 10^2$ measured by Monzyk and Crumbliss at 25 °C and $I = 1.1$ M ($HClO_4$/$NaClO_4$).[20] The kinetic study demonstrates that in the formation of the 1:1 complexes the reactive Iron(III) form is $FeOH^{2+}$. Although a small $Fe(H_2O)_6^{3+}$ contribution could be expected,[20] and experimentally found for instance for Iron(III)/salicylate systems,[45] this was found to be negligible over the concentration range explored in the present investigation. The k_1 value for Fe/BHA reported in Table 3 compares fairly well with the $4.3 \times 10^3\ M^{-1}\ s^{-1}$ value by Monzyk and Crumbliss at $I = 2$ M.[20] According to the conclusions accepted[46] about complex formation reactions at $Fe(H_2O)_5OH^{2+}$, the formation of the 1:1 chelate, represented as a single reaction for the sake of simplicity (reaction 10 or reaction (15) for Iron(III)/SHA), is in effect composed by the sequence shown in Scheme 5. where step (1) represents the formation of the $(OH)Fe(H_2O)_5$, H_2L outer-sphere complex, which converts to the inner-sphere monodentate complex $(OH)Fe(H_2O)_4H_2L$ in the rate-determining step (2), according to the dissociative I_d mechanism first proposed by Eigen and Tamm.[47] Therefore, internal proton transfer, removal of a second water molecule and ring closure rapidly occur in step (3), which leads to formation of the stable chelate $Fe(H_2O)_4HL$.

Iron(III)/SHA. Still more important for the focus of the present work are the results concerned with the binding of the second Iron(III) ion to SHA. According to the reaction Scheme 3, the species $[Fe_2OHH_2L]^{4+}$ can form by direct attack of H_3L to the dimer $Fe_2(OH)_2^{4+}$ or/and by reaction of the $FeOH^{2+}$ monomer with the FeH_2L monochelate. The equilibrium constant of the latter reaction is $K_C = K_D K_2/K_1 = 5.2\ M^{-1}$. This finding indicates that the formation of $Fe_2OHH_2L^{4+}$ from FeH_3L^{3+} and $FeOH^{2+}$ is largely disfavored with respect to step (16), which involves the direct interaction of the dimer with H_3L. It should be mentioned here that direct attack of $Fe_2(OH)_2^{4+}$ to ligands were observed in the case of Tiron,[48] tropolone,[49] and 5-nitro tropolone.[50] The first act of the binding process appears to occur with the same mode of activation, since the values of the rate constants for this step are similar: $5.1 \times 10^3\ M^{-1}\ s^{-1}$ for Tiron,[48] $2.1 \times 10^4\ M^{-1}\ s^{-1}$ for Tropolone,[49] $3 \times 10^4\ M^{-1}\ s^{-1}$ for 5-nitrotropolone,[50] and

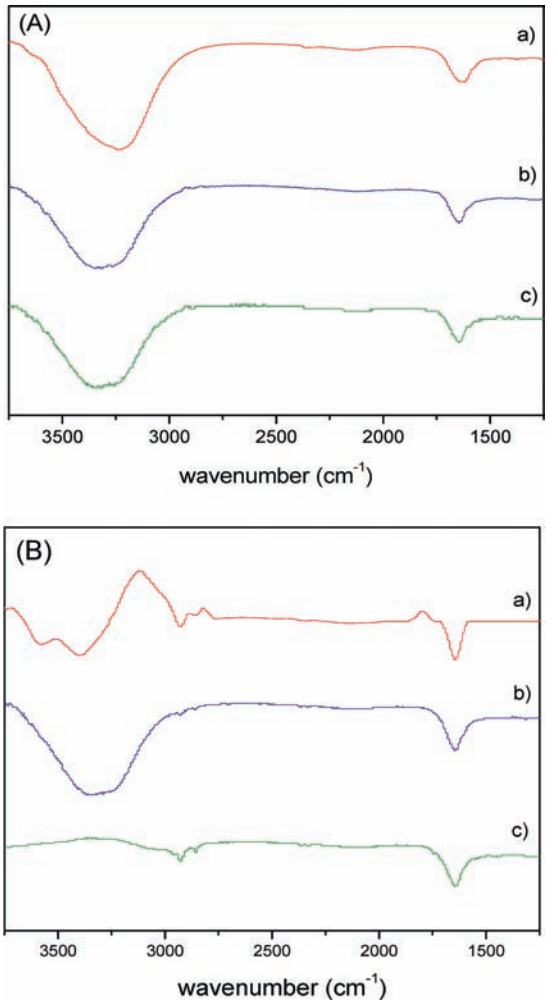

Figure 12. FTIR spectra of the investigated systems; $[H^+] = 0.022$ M, $I = 1$ M ($HClO_4$/$NaClO_4$), $T = 298$ K. [BHA] or [SHA] = 5×10^{-3} M (A) the Iron(III)/BHA system: (a) BHA, (b) Iron(III):BHA = 1:1, (c) Iron(III):BHA = 2:1; (B) the Iron(III)/SHA system: (a) SHA, (b) Iron(III):SHA = 1:1, (c) Iron(III):SHA = 2:1.

Scheme 4

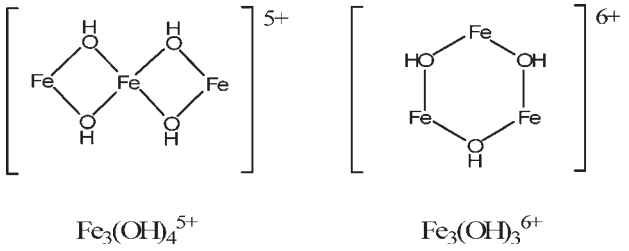

$1.5 \times 10^4\ M^{-1}\ s^{-1}$ for SHA (this work). A dimeric intermediate, structured as in Scheme 6, has been proposed to explain the kinetic behavior of the Iron(III)/Tiron system:[48] where the two Iron(III) units are linked through a μ-OH and a μ-OC bridge. A similar structure can be proposed for the species $Fe_2OHH_2L^{4+}$ formed in reaction (16). The two dimeric forms are unstable[48−51] but, whereas the Iron(III)/Tiron structure decomposes to give $FeL+FeOH^{2+}$, in the Iron(III)/SHA system the $Fe_2OHH_2L^{4+}$

dx.doi.org/10.1021/ic201112j |Inorg. Chem. 2011, 50, 10152–10162

Scheme 5

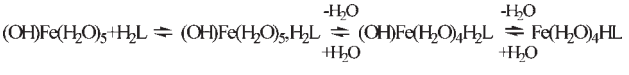

Scheme 6

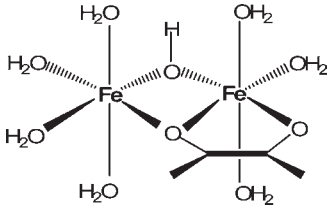

ion evolves toward the more stable Fe_2L^{3+} structure by the slow reaction (17), as supported by the titration, kinetic, and IR experiments. Our titrations show that the affinities of Iron(III) for the O,O and O_P,N sites are very different ($K_{ML} \gg K_{M2L}$); since the value of K_{ML} for SHA and BHA are similar, we can conclude that Iron(III) manifests a preference for the O,O site. The stabilization of the second iron atom within a single ligand molecule is provided by the O_P,N site which, even though is not able to directly bind divalent metal ions,[31] displays an appreciable affinity toward Iron(III). Note that in the case of BHA any attempt to observe the presence of the 2:1 complex inexorably failed.

It is also useful to discuss here the ability of SHA to form a dinuclear complex with Iron(III) in the context of its ability to form metallacrowns. Actually, the hydroxamate and the phenolate residues present in SHA turn this molecule into a dinucleating agent. Moreover, the dinuclear complex, is stabilized owing to the high charge density of the Fe^{3+} ion, which facilitates the removal of protons from the O_P,N site. The ability of eq 12 to represent the K_{2app} versus $[H^+]$ dependence, the linear increase of the rate of decomposition of the dinuclear complex on rising $[H^+]$, and the FTIR spectra, all lead to the important conclusion that both Iron(III) ions are chelated by the two SHA reaction sites, whereas the ligand is fully deprotonated, in agreement with the structure shown in Figure 1. This structure displays the sequence Fe(A)−N−O−Fe(B), which constitutes the network linking the metals contained in metallacrown rings such as 12-MC-4.[25,30]

Once the basic unit depicted in Figure 1, M_2L, has been formed, the next step could be the linkage of a further ligand molecule to M_2L to give the M_2L_2 dimer. Note that recent ITC titrations of the Cu^{2+}/(*S*)−α-aminohydroxamic acid system, made in our laboratory, provided calorimetric curves displaying a jump at the stoichiometric ratio M:L = 2:1, which suggests formation of the M_2L species. The rates of formation of ML, M_2L, and M_2L_2 depend on the metal nature.[46] These processes can be extremely fast as, for instance, in the case of Cu^{2+} ion. On the other hand, the overall rate of metallacrown formation appears to be a relatively slow process. This feature hints at the possibility that the crown formation could involve the aggregation of two dimer molecules to give a more complex species. An alternative route to the formation of the crown would involve the union of a $Cu(H_2O)_4^{2+}$ ion to M_2L_2, but this process would be very fast, and therefore a kinetically distinguishable process. In this regard, the kinetic approach could in principle provide important information not only on the mode of formation of the basic unit but also on the mechanism of crown assembly and even on the mechanism of metal binding to the central cavity and/or on the metal exchange process.

CONCLUSIONS

The kinetic study of the interaction of Iron(III) with BHA and SHA required a rather complete knowledge of the hydrolysis and self-aggregation processes of Iron(III). The values of reaction parameters for these processes agree pretty well with literature data. Moreover, through the elucidation of the mechanism of formation/dissociation of the trimer, the ambiguity existing about the structure of this species has been solved.

The main aim of this paper was to prove the existence of a dinuclear complex (M_2L) formed by the reaction of Iron(III) with salicylhydroxamic acid (SHA). The formation of this complex has been demonstrated by spectrophotometric titration, stopped-flow kinetics and FTIR experiments. The binding of the second Iron(III) atom involves the deprotonation of the SHA N−H site, and the formation of M_2L provides the rationale for the building of complex structures as metallacrowns. The results obtained in the kinetic study of formation/decomposition of M_2L enabled us to describe for the first time the microscopic processes which are at the basis of the formation of the building blocks of the metallacrowns. Not only do the data here presented provide a valuable basis for further kinetic studies on Iron(III) base metallacrowns, but they also suggest what microscopic interactions can be taken into account to describe the routes to bigger metallacrowns.

ASSOCIATED CONTENT

Supporting Information. UV−vis spectra of $Fe(ClO_4)_3$; Lambert−Beer plots; kinetic trace showing formation of Iron(III) aggregates other than dimer and trimer; titration curves of the Iron(III)/SHA system; kinetic curves for Iron(III) binding to BHA and SHA; derivation of the speciation curve for the $Fe(ClO_4)_3$/$[H^+]$ system; derivation of the relaxation times for a system of two coupled reactions; derivation of the rate equations for the Iron(III)/SHA system; derivation of the relationship between the apparent binding constant, K_{app}, and the individual binding constant, *K*; derivation of the fast relaxation time for Iron(III) dimerization. This material is available free of charge via the Internet at http://pubs.acs.org.

AUTHOR INFORMATION

Corresponding Authors
*E-mail: ferdi@dcci.unipi.it, begar@ubu.es.

ACKNOWLEDGMENT

The financial support by Ministerio de Educación y Ciencia, Project CTQ2009-13051/BQU, supported by FEDER, Junta de Castilla y León, Projects BU-013A-09 and GR257 and Universidad de Burgos with funding by Caja de Burgos, Spain.

REFERENCES

(1) Winkelmann, G.; van der Helm, D., Neilands, J. B., Eds.; *Iron Transport in Microbes, Plants, and Animals*; VCH: Weinheim, Germany, 1987; p 533.

(2) Albrecht-Gary, A. M.; Crumbliss, A. L. *Met. Ions Biol. Syst.* **1998**, *35*, 239–327.
(3) Natarajan, R.; Nirdosh, I. *Int. J. Miner. Process.* **2009**, *93*, 284–288.
(4) Sreenivas, T.; Padmanabhan, N. P. H. *Colloids Surf., A* **2002**, *205*, 47–59.
(5) Codd, R. *Coord. Chem. Rev.* **2008**, *252*, 1387–1408.
(6) Muri, E. M. F.; Nieto, M. J.; Sindelar, R. D.; Williamson, J. S. *Curr. Med. Chem.* **2002**, *9*, 1631–1653.
(7) Lou, B.; Yang, K. *Mini-Rev. Med. Chem.* **2003**, *3*, 609–620.
(8) Zamora, R.; Grzesiok, A.; Weber, H.; Feelisch, M. *Biochem. J.* **1995**, *312*, 333–339.
(9) Mishra, R. C.; Tripathi, R.; Katiyar, D.; Tewari, N.; Singh, D.; Tripathi, R. P. *Bioorgan. Med. Chem.* **2003**, *11*, 5363–5374.
(10) Apfel, C.; Banner, D. W.; Bur, D.; Dietz, M.; Hirata, T.; Hubschwerlen, C.; Locher, H.; Page, M. G. P.; Pirson, W.; Rosse, G.; Specklin, J. L. *J. Med. Chem.* **2000**, *43*, 2324–2331.
(11) Holland, K. P.; Elford, H. L.; Bracchi, V.; Annis, C. G.; Schuster, S. M.; Chakrabarti, D. *Antimicrob. Agents Chemother.* **1998**, *42*, 2456–2458.
(12) Tsafack, A.; Golenser, J.; Libman, J.; Shanzer, A.; Cabantchik, Z. I. *Mol. Pharmacol.* **1995**, *47*, 403–409.
(13) Golenser, J.; Tsafack, A.; Amichai, Y.; Libman, J.; Shanzer, A.; Cabantchik, Z. I. *Antimicrob. Agents Chemother.* **1995**, *39*, 61–65.
(14) Bouchain, G.; Delorme, D. *Curr. Med. Chem.* **2003**, *10*, 2359–2372.
(15) Steward, W. P. *Cancer Chemother. Pharmacol.* **1999**, *43*, S56–S60.
(16) Brammer, R.; Buckels, J.; Bramhall, S. *Int. J. Clin. Pract.* **2000**, *54*, 373–381.
(17) Holms, J.; Mast, K.; Marcotte, P.; Elmore, I.; Li, J. L.; Pease, L.; Glaser, K.; Morgan, D.; Michaelides, M.; Davidsen, S. *Bioorg. Med. Chem. Lett.* **2001**, *11*, 2907–2910.
(18) Exner, O.; Hradil, M.; Mollin, J. *Collect. Czech. Chem. Commun.* **1993**, *58*, 1109–1121.
(19) García, B.; Secco, F.; Ibeas, S.; Muñoz, A.; Hoyuelos, F. J.; Leal, J. M.; Senent, M. L.; Venturini, M. *J. Org. Chem.* **2007**, *72*, 7832–7840 and references therein.
(20) Monzyk, B.; Crumbliss, A. L. *J. Am. Chem. Soc.* **1979**, *101*, 6203–6213.
(21) Tegoni, M.; Remelli, M. *Coord. Chem. Rev.* accepted manuscript, DOI: 10.1016/j.ccr.2011.06.007.
(22) Kurzak, B.; Farkas, E.; Glowiak, T.; Kozlowski, H. *J. Chem. Soc., Dalton Trans.* **1991**, 163–167.
(23) Psomas, G.; Stemmler, A. J.; Dendrinou-Samara, C.; Bodwin, J. J.; Schneider, M.; Alexiou, M.; Kampf, J. W.; Kessissoglou, D. P.; Pecoraro, V. L. *Inorg. Chem.* **2001**, *40*, 1562–1570.
(24) Gibney, B. R.; Pecoraro, V. L. *Inorg. Syn.* **2002**, *33*, 70–74.
(25) Pecoraro, V. L.; Stemmler, A. J.; Gibney, B. R.; Bodwin, J. J.; Wang, H.; Kampt, J. W.; Barwinski, A. Metallacrowns: A New Class of Molecular Recognition Agents. In *Progress in Inorganic Chemistry*; Pergamon Press: New York, 1996; Vol. 45, pp 83−177.
(26) Tegoni, M.; Furlotti, M.; Tropiano, M.; Lim, C. S.; Pecoraro, V. L. *Inorg. Chem.* **2010**, *49*, 5190–5201.
(27) Lim, C.-S.; Jankolovits, J.; Zhao, P.; Kampf, J. W.; Pecoraro, V. L. *Inorg. Chem.* **2011**, *50*, 4832–4841.
(28) Wang, S.; Kong, L.; Yang, H.; He, Z.; Jiang, Z.; Li, D.; Zeng, S.; Niu, M.; Song, Y.; Dou, J. *Inorg. Chem.* **2011**, *50*, 2705–2707.
(29) Boron, T. T., III; Kampf, J. W.; Pecoraro, V. L. *Inorg. Chem.* **2010**, *49*, 9104–9106.
(30) Mezei, G.; Zaleski, C. M.; Pecoraro, V. L. *Chem. Rev.* **2007**, *107*, 4933–5003.
(31) García, B.; Gonzalez, S.; Hoyuelos, F. J.; Ibeas, S.; Leal, J. M.; Senent, M. L.; Biver, T.; Secco, F.; Venturini, M. *Inorg. Chem.* **2007**, *46*, 3680–3687.
(32) Castellan, G. W. *Ber. Bunsen-Ges.* **1963**, *67*, 898–908.
(33) D'Amico, M. L.; Paiotta, V.; Secco, F.; Venturini, M. *J. Phys. Chem. B* **2002**, *106*, 12635–12641.
(34) García, B.; Ibeas, S.; Hoyuelos, F. J.; Leal, J. M.; Secco, F.; Venturini, M. *J. Org. Chem.* **2001**, *66*, 7986–7993.
(35) Rossotti, F. J. C.; Rossotti, H. *The determination of stability constants*; Mc Graw-Hill Book Company Inc.: New York, 1961; p 425.
(36) Artemenko, A. I.; Anufriev, E. K.; Tikunova, I. V. *Zh. Prikl. Spektrosk.* **1980**, *32*, 641–647.
(37) Kaczor, A.; Szczepanski, J.; Vala, M.; Proniewicz, L. M. *Phys. Chem. Chem. Phys.* **2005**, *7*, 1960–1965.
(38) Baes, C. F.; Mesmer, R. E. *The hydrolysis of cations*; John Wiley & Sons: New York, 1976; p 489.
(39) Davies, C. W. *Ion Association*; Butterworths: London, 1962; p 190.
(40) Sommer, B. A.; Margerum, D. W. *Inorg. Chem.* **1970**, *9*, 2517–2521.
(41) Wendt, H. *Inorg. Chem.* **1969**, *8*, 1527–1528.
(42) Guentelberg, E. *Z. Physik. Chem.* **1926**, *123*, 199–247.
(43) Po, H. N.; Sutin, N. *Inorg. Chem.* **1971**, *10*, 428–431.
(44) Prue, J. E. *Ionic Equilibria*; Pergamon Press: Oxford, U.K., 1966; p 115.
(45) Mentasti, E.; Secco, F.; Venturini, M. *Inorg. Chem.* **1982**, *21*, 602–606.
(46) Burgess, J. *Metal ions in solution*; Ellis Horwood Limited: Chichester, U.K., 1978; p 481.
(47) Eigen, M.; Tamm, K. *Z. Elektrochem. Angew. Phys. Chem.* **1962**, *66*, 107–121.
(48) Chatlas, J.; Jordan, R. B. *Inorg. Chem.* **1994**, *33*, 3817–3822.
(49) Secco, F.; Venturini, M.; Fanelli, N. *Ann. Chim.-Rome* **1999**, *89*, 129–136.
(50) Secco, F.; Venturini, M. *Polyhedron* **1999**, *18*, 3289–3293.
(51) Lente, G.; Fabian, I. *Inorg. Chem.* **2002**, *41*, 1306–1314.